Intracavity third-harmonic generation in Si:B pumped by intense terahertz pulses

Meng, F.; Thomson, M. D.; Ul-Islam, Q.; Klug, B.; Pashkin, O.; Schneider, H.; Roskos, H. G.;

Originally published:

August 2020

Physical Review B 102(2020), 075205

DOI: https://doi.org/10.1103/PhysRevB.102.075205

Intracavity third-harmonic generation in Si:B pumped by intense terahertz pulses

Fanqi Meng,[1, a)] Mark D. Thomson,[1] Qamar ul-Islam,[1] Bernhard Klug,[1] Alexej Pashkin,[2] Harald Schneider,[2] and Hartmut G. Roskos[1, b)]

[1)] *Physikalisches Institut, Goethe-Universität Frankfurt, 60438 Frankfurt am Main, Germany*

[2)] *Institute of Ion Beam Physics and Materials Research, Helmholtz-Zentrum Dresden-Rossendorf, 01328 Dresden, Germany*

(Dated: 17 June 2020)

We observe third-harmonic generation (THG) in boron-doped silicon (Si:B) upon pumping with picosecond 1.56-THz pulses from a free-electon laser with a peak electric field strength of up to 12 kV/cm. The measurements are performed at cryogenic temperatures where the majority of holes are bound to the acceptor dopants. The dependence of the THG on the pump intensity exhibits a threshold-free power-law behavior with an exponent close to 4. The observations can be explained by THz emission by free holes accelerated in the non-parabolic valence band, under the assumption that the density of free holes increases with the pump intensity. A quantitative treatment supports that these carriers are generated by impact ionization, initiated by the population of thermally ionized carriers , as opposed to direct tunneling ionization. In addition, we also observe intracavity THG by embedding the Si:B in a one-dimensional photonic crystal cavity. The THG efficiency is increased by a factor of eight due to the field enhancement in the cavity, with the potential to reach a factor of more than 100 for pump pulses with a spectrum narrower than the linewidth of the cavity resonance.

I. INTRODUCTION

While dopants in semiconductors are well-known for their role of providing charge carriers in room-temperature semiconductor devices, many ongoing studies are devoted to dopant physics at low temperature, where the charges remain bound to their parent ions such that the dopants represent energy-scaled hydrogen-like atomic entities within a solid-state host[1,2]. Topics of such investigations include the nonlinear optical properties of the dopants[3,4], the possibility to realize THz gain media with them[5], as well as the coherent control of the dopant states for quantum information processing[6,7].

This contribution is devoted to the nonlinear dynamics of holes following ionization of dopants and subsequent acceleration of the freed holes in the strong radiation field of intense electromagnetic pulses. The work has been motivated by studies of strong electromagnetic-field phenomena of dilute gas atoms, which led to the observation of frequency multiplication upon recollision of the photo-ionized electrons with the parent ions[8–12]. We extend such studies to atoms dilutely distributed in the crystalline matrix of a solid semiconductor.

We study Si:B at low temperature with high-field excitation by terahertz (THz) pulses from a free-electron laser (FEL). Although the photon energy of 6.45 meV is much lower than the $1\Gamma_8^+ \rightarrow 1\Gamma_8^-$ ($1S_{3/2} \rightarrow 2P_{3/2}$) transition energy at 30.6 meV, dopant atoms are ionized in the strong radiation field of up to 12 kV/cm. We observe THG exclusively in the doped material, where the pump intensity dependence indicates a third-order nonlinearity with an intensity-dependent $\chi^{(3)}$ coefficient. This suggests that the THG is mediated by carriers released from dopants in the valence band, whereby the carrier density increases as a function of the field strength. While in principle several physical mechanisms can contribute, a comparison of their respective field dependences suggests that the additional carriers are generated by impact ionization (as opposed to tunnel ionization), a process initiated by the carriers which are initially present due to thermal activation. No evidence for high-harmonic generation (HHG) by recollision is identified.

Moreover, we exploit the field enhancement in a one-dimensional photonic crystal (1D-PC) cavity to enhance the THG conversion efficiency with cavity-resonant pumping. Such 1D PC cavities have been introduced in the THz range for a range of applications, e.g., as switches and modulators[13], and for the study of strong light-matter interaction[14,15]. Here, we achieve an increase in the THG efficiency by a factor of up to eight relative to the free-standing Si:B sample, and predict that an enhancement of over one hundred is possible if the spectral width of the pump pulse were to be reduced to better match the cavity resonance.

II. EXPERIMENTAL

The experimental setup is depicted in Fig. 1a. The Si:B sample was positioned in a liquid-helium cryostat at a temperature of 10 K. Intense THz pulses from the FELBE facility of the Helmholtz-Zentrum Dresden-Rossendorf were employed as pump radiation. The FELBE source delivers transform-limited multi-cycle terahertz pulses which are tunable from 1.2 THz up to 75 THz at a pulse repetition rate of 13 MHz. For our experiments, we chose a radiation frequency of 1.56 THz; the spectral width of the pulses was 22.4 GHz (full-width-at-half-maximum, FWHM). This corresponds to a temporal intensity FWHM of 17 ps, assuming transform-limited pulses and using a numerical inverse Fourier transformation of the measured amplitude spectrum (rms time-bandwidth product 1.46 relative to Gaussian pulse/spectrum). The incoming radiation was focused onto

[a)] Electronic mail: f.meng@physik.uni-frankfurt.de.

[b)] Electronic mail: roskos@physik.uni-frankfurt.de.

the sample with an off-axis paraboloidal mirror with a 50.8-mm effective focal length, to obtain a focal beam diameter of $2w \sim 400$ μm (and a corresponding Rayleigh range of $z_0 = n\pi w^2/\lambda_0 \sim 2$ mm in the Si sample, where $n = 3.42$ is the refractive index and λ_0 is the vacuum wavelength of the THz radiation). The generated higher-harmonic radiation was collected and collimated with a second paraboloidal mirror and guided to a Fourier Transform Infrared Spectroscopy (FTIR) setup (employing a high-resisitivity (HR) polished Si beamsplitter), where the field correlation signal was measured with a liquid-helium-cooled bolometer (Infrared Laboratories LN-6/C, NEP: 1.28×10^{-13} W Hz$^{-1/2}$), with a frequency resolution of 20 GHz set by the scan range. In front of the sample, a low-pass filter consisting of a 2-mm-thick fused silica plate was positioned in the FEL beam to absorb the intrinsic higher harmonics of the FEL. Following the sample, two high-pass filters (multi-layer metal-mesh filters HP74cm^{-1} and HP100cm^{-1} from QMC Instruments Ltd.) were employed to strongly reduce the transmitted fundamental pump intensity (with a residual transmittance of 1.1×10^{-7}) in order to improve the dynamic range for the HHG signals. The combined power transmittance of the filter pair is 0.7, 0.07 and 0.08 at the third, fifth and seventh harmonics, respectively. The broadband FTIR setup supports a bandwidth of more than 10 THz, the dynamic range at different frequencies depending on the transmission characteristics of the high-pass filters.

The specimen-under-test was a commercial Si:B sample (purchased from MTI Corp.) with a dopant density of 5×10^{16} cm^{-3} and a wafer thickness of 275 μm. The dopant density was chosen to be as high as possible to obtain sufficiently strong signals, but low enough to remain at the onset of inter-dopant interactions well below the Mott density of impurity-band formation[16,17]. This is demonstrated by the linear transmission spectra shown in Fig. 1b, which were measured by FTIR spectroscopy at the indicated temperatures from 5-150 K. The spectra exhibit the expected series of discrete ground-state transition lines at 7.39, 8.41 and 9.67 THz of ground-state B dopants in Si[2,18]. Compared with the lineshapes observed in the case of samples with a dopant density below 5×10^{15} cm^{-3},[2,16] the three lines are broadened, but remain clearly separated from each other at 5 K. With rising temperature, they weaken due to thermal ionization and broaden due to interaction with the free-hole plasma, while the background transmission decreases due to both the Drude absorption of the free carriers (from the low-frequency side) and red-shifted continuum absorption by dopants in thermally activated bound excited states.

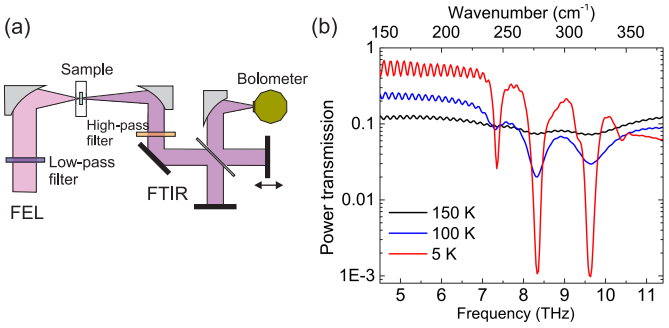

FIG. 1. (a) Experimental setup for the HHG measurements. The sample is positioned in a cryostat to enable temperature control. (b) Linear power transmission spectra of Si:B at three temperatures (150 K, 100 K and 5 K), measured by FTIR spectroscopy. The ringing, most pronounced at low frequency, arises from multiple-reflection interference in the Si:B sample.

III. RESULTS

A. THG from free-standing Si:B

Figure 2a presents transmission spectra of the Si:B sample recorded upon illumination with strong THz radiation. The spectra consist of transmitted (leaking) FEL radiation and HHG radiation emitted from the sample. In the curves taken at three different pump pulse energies, one observes line features, the most promiment ones being at 3.12, 4.68 and 6.24 THz in addition to the residual pump light at the fundamental frequency of 1.56 THz. The lines at 3.12 THz and 6.24 THz are the second and fourth harmonics of the pump light, their intensities are found to be directly proportional to the pump intensity.The origin of the additional weaker features in the spectrum such as the broad structure between 2.0 and 4.0 THz and the line at 6.9 THz is unknown to us. However, all features except for the line at 4.68 THz originate from the FEL itself. This was confirmed with measurements taken with a nominally undoped HR Si specimen in the beam path (sample with a room-temperature specific resistance >12 kΩcm purchased from University Wafer Inc.), as also included in Fig. 2a (vertically shifted green curve), which exhibits all of the above-mentioned features except for the line at 4.68 THz. This signal, at the third harmonic of the pump frequency, can hence be attributed to the boron dopants of the Si:B sample. Its intensity exhibits a superlinear pump-power dependence, investigated in detail in the following. Note that the absence of a third-harmonic signal in the reference measurement with the undoped sample proves that this signal cannot originate from the bound electrons of the Si atoms[19]. We also note that no spectral features were observed here at the 5th and the 7th harmonic frequencies (7.80 and 10.92 THz). The implications will be discussed in Sec. IV.

Figure 2b displays the measured pulse intensity $I_{3\omega}$ of the third-harmonic line for seven values of the pulse energy of the pump pulses, from 5.5 to 31.2 nJ (corresponding to a peak pump intensity I_ω ranging from 0.17 to 0.95 MW/cm^2, all measured in front of the sample). The error bars indicate the FEL power fluctuations. The dependence can be fitted with a power law $I_{3\omega} \propto I_\omega^\eta$ with $\eta = 3.9$, as shown by the black dash-dotted line in Fig. 2b. The exponent η is clearly larger than the value $\eta = 3$ expected for a third-order nonlinearity with a constant $\chi^{(3)}$ susceptibility, as was previously reported for far-infrared THG experiments on doped Si at room temperature[20], where all dopants (concentration n_d) were thermally ionized and one observes $\chi^{(3)} \propto n_d$. The susceptibility evidently must

be taken as pump-power-dependent, which we write as:

$$I_{3\omega} = \beta \left(\chi^{(3)}_{eff}(I_\omega)\right)^2 \cdot I^3_\omega \,, \qquad (1)$$

where β is a constant proportionality factor. With the data of Fig. 2b, and the relationship $I_\omega = (n+1)^2 \varepsilon_0 c_0 E^2_\omega/8$, which connects I_ω (measured in front of the sample) with the peak electric field E_ω within the sample (ε_0: vacuum permittivity, c_0: vacuum speed of light), we can derive the dependence of $\chi^{(3)}_{eff}(I_\omega)$ on E_ω, shown by the blue triangles in Fig. 2c.

The rise of the susceptibility with the pump field strength suggests that the entities, responsible for the nonlinearity, increase in number with rising field strength. This strongly suggests free holes to be the origin of the nonlinearity, such that

$$\chi^{(3)}_{eff}(I_\omega) = \chi^{(3)} \cdot n_h(I_\omega), \qquad (2)$$

with $n_h(I_\omega)$ being the pump-dependent density of free holes.

In the following, we discuss three mechanisms which could be considered to explain the field-dependent susceptibility in Fig. 2c: (i) ionization of the dopants by multiphoton absorption, (ii) radiation-field-induced tunneling processes, and (iii) impact ionization initiated by a residual population of thermally ionized free holes which are accelerated in the pump field.

With regard to multiphoton ionization, we can refer to Ref. 3, where two- and three-photon THz absorption was studied experimentally and theoretically for the case of phosphorus dopants in Si:P – a system which has quite similar dopant-related optical properties as Si:B. It was found that the observation of three-photon transitions from the 1s ground state requires a pulse intensity of at least 17 MW/cm^2 (for a two-photon process, it is ten times less). This is much more than was available in our experiments (see Fig. 2b, upper scale). In addition, one would need at least a five-photon absorption process for such an excitation in Si:B with 1.56-THz photons, which would require a much higher intensity. Based on these numbers, we can rule out multiphoton absorption as relevant for the increase of the hole density in our measurements.

Considering now direct tunnel ionization, it is useful to follow the procedures applied in the studies of ionization of atomic gasses, and to compare the expected significance of tunneling relative to multiphoton ionization with the help of the Keldysh parameter[21] γ (see Appendix, Section VI A). Here we estimate $\gamma = 2.8$ for light holes (and $\gamma = 4.85$ for heavy holes) for a radiation field strength of 10 kV/cm, typical for our experiments. As $\gamma > 1$, this implies that multiphoton ionization is expected to dominate over tunneling ionization. As the former has already been found to be insignificant, so apparently is also the latter. Another argument against tunneling ionization is the electric-field dependence to be expected for the hole density n_h. The magenta-colored curve in Fig. 2c displays the field trend of Δn, the hole density created by tunnel ionization as calculated with the expressions given in Sec. VI B. As can be seen, the electric field dependence is far more nonlinear than that of the experimentally determined $\chi^{(3)}_{eff}$, even when one attempts to match the offset and scale

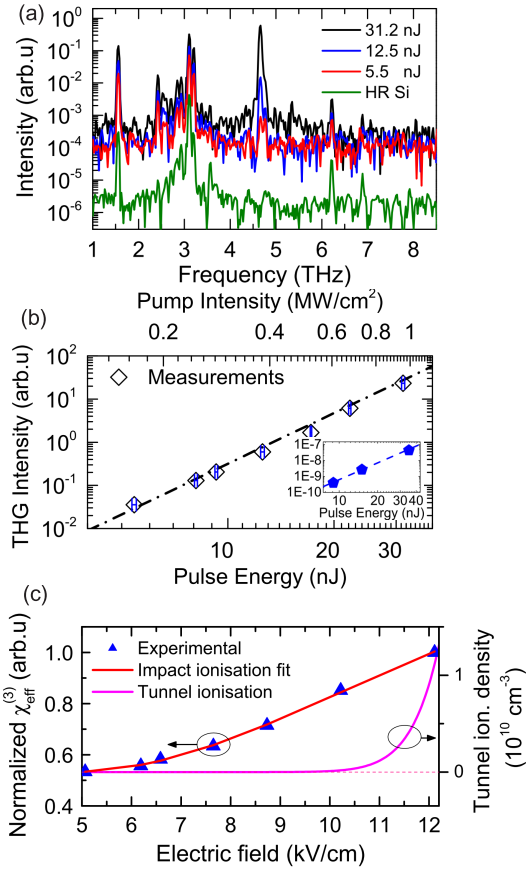

FIG. 2. (a) Transmittance/emittance spectra of the Si:B sample exposed to 1.56-THz radiation at the three pump pulse energies of 5.5, 12.5 and 31.2 nJ (power measured directly in front of the sample). Also included is the transmittance spectrum of the undoped HR Si sample for a pump pulse energy of 21.7 nJ (green curve, scaled down by a factor of 100 for better visibility in the logarithmic plot). (b) Black open diamonds: Measured THG intensity as a function of the pulse energy of the FEL beam, the error bars represent the power fluctuation of the FEL. Black dash-dotted line: Power-law dependence with an exponent of 3.9. The inset shows the results of a THG measurement using the TELBE facility where the pulse repetition rate is only 50 kHz (leading to reduced sample heating). The blue pentagons represent the measured THG intensity and the blue dashed line a power law with an exponent of 3.6. (c) Blue triangles: Normalized effective nonlinear susceptibility $\chi^{(3)}_{eff}$ as a function of the electric radiation field E_ω of the pump pulse in the sample. Red curve: Simulated $\chi^{(3)}_{eff} = \chi^{(3)} \cdot n_h$ due to impact ionization. Both are normalized to the respective values obtained at 12 kV/cm. Magenta-colored curve: Estimated density of light holes created by tunneling ionization.

to the data, which supports the conclusion that direct tunneling cannot be the main contribution to the ionization in our experiments.

This leaves the third mechanism, impact ionization, initiated by thermally ionized free holes. That this is an effective ionization mechanism of shallow dopants at low temperature in moderately strong applied DC fields (before tunneling ionization sets in) has been known for a long time[22–24]. Impact

ionization of shallow dopants by THz radiation pulses has apparently not been studied yet[25], in contrast to the case of interband impact ionization in narrow-bandgap semiconductors exposed to intense THz and infrared radiation[26–29]. The theoretical treatment of this interband excitation involves accounting for the high-energy tail of the energy distribution of existing free carriers accelerated by the radiation field. This leads to a simple expression for the density of impact-generated charge carriers, which turns out to be applicable for the analysis of our data[26,29]:

$$\frac{\Delta n}{n_0} = A \exp\left(-\frac{E_0^2}{E_\omega^2}\right), \tag{3}$$

where A is a factor that weakly depends on the pump electric field, n_0 is the initial density of free carriers at the sample temperature, and E_0 is a characteristic electric field dependent on the radiation frequency. We will discuss the applicability of this expression for shallow impurities and the characteristics of the FELBE THz radiation pulses in Sec. IV A. For now, we apply this expression assuming A to be constant over the field range of our measurements, insert it into Eq. (2) in the term for the hole density $n_h = n_0 + \Delta n$, and fit the equation to the values of $\chi^{(3)}_{eff}$ extracted from the measurements. For E_0 =11.3 kV/cm, and $A = 0.92$, we obtain the results shown by the red curve in Fig. 2c, which reproduces the experimental data very well. We note that both impact and tunnel ionization rates have an exponential field dependence in their low-field regimes, i.e. $E \ll E_0 = 11.3$ kV/cm (Eq. (3)) and $E \ll \alpha_E = 261$ kV/cm (see Eq.s (5-8) below), respectively, with both going into a polynomial-like saturation at higher fields $E \gtrsim E_0, \alpha_E$. On this basis, only impact ionization can reproduce the moderate field dependence of the experimental data in Fig. 2c in our field range.

While this good agreement supports the notion that the THG of our experiments originates indeed from a $\chi^{(3)}$-nonlinearity of free holes in the valence band, we have yet to identify the origin of the nonlinearity itself. Referring to studies of the free-carrier nonlinearity of various doped semiconductors at room temperature[20,30–33], one finds that possible contributions to the nonlinearity may come from both the nonparabolicity of the energy band in reciprocal space[20,31–33] and from the nonlinear dependence of the free-carrier relaxation time on momentum[20,30] (for kinetic-energy-dependent scattering of holes in group-IV semiconductors, see e.g. Ref. 34). With the data available from our experiments, we cannot presently conclude which of the two contributions may dominate in our case (see discussion in Sec. IV A).

We finally address the question whether the dependence of the nonlinearity on the density of holes may simply result from thermal ionization of bound dopants due to sample heating by the THz pulse train. Since the repetition rate of the FELBE pulses is high (13 MHz), absorbed radiation energy could lead to an elevated sample temperature, at which radiation heating and energy loss by thermal diffusion are again in balance. However, an analysis of the absorbed power and heat diffusion in the sample (see Sec. VI C) tends to rule this out. To test experimentally for such a contribution, we performed additional THG measurements em-

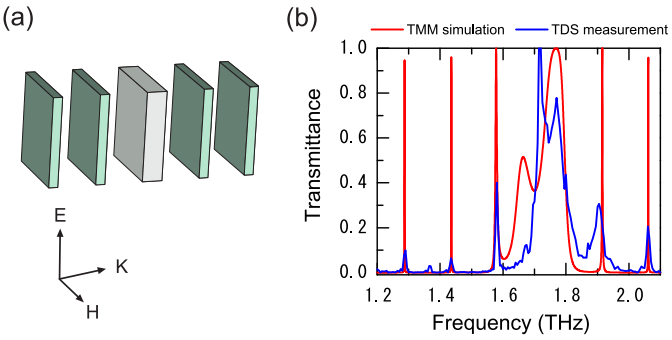

FIG. 3. (a) Scheme of the 1D PC cavity. (b) Blue line: Transmittance spectrum of the 1D PC cavity at 20 K measured by THz time-domain spectroscopy (TDS); red line: transmittance spectrum calculated with the transfer matrix method (TMM). The spectra are as simulated respectively measured, without normalization.

ploying a different pump source – the new superconducting radio-frequency accelerator-based superradiant THz source (TELBE at HZDR)[30]. This system operates at a repetition rate of only 50 kHz, a rate 260 times lower than that of FELBE, such that any heat accumulation will be significantly reduced. The measured THG intensity as a function of the pump pulse energy is shown in the inset of Fig. 2b for the same energy range of the pump pulses as in the experiments discussed above. Again, the intensity of the third-harmonic signal increases with the pump pulse energy, albeit with a lower power-law exponent of $\eta = 3.6$ (instead of $\eta = 3.9$). The exponent $\eta > 3$ is again evidence for an electric-field-induced carrier multiplication, while the somewhat lower η value may well be due to the different pump radiation frequency (0.3 THz) used in the TELBE experiment (and hence a different value of E_0 in Eq. (3) above).

B. Intracavity THG from Si:B

In order to investigate intracavity THG, a 1D PC cavity was constructed which consisted of a so-called defect layer between two Bragg mirrors[15]. A sketch of the cavity is shown in Fig. 3a. The 275-μm-thick Si:B sample served as the defect layer, and two identical pairs of unit structures consisting of a 50-μm-thick slab of HR Si and a 46-μm-wide air gap as Bragg mirrors on both sides of the defect layer. We calculated the linear transmittance spectrum of the cavity using the transfer matrix method. The result is shown by the red line in Fig. 3b. The spectrum consists of equally spaced narrow-band cavity resonances within the stop-bands and a much broader high-transmittance region in the range 1.6-1.8 THz between the stop-bands. For the cavity mode at 1.58 THz, chosen for the experiments below, the theoretical intracavity field enhancement factor $r_E = 4.6$ (directly on resonance, at the standing-wave antinodes in the defect layer), although as discussed below, this is the continuous-wave (CW) limit and the achievable field enhancement for a pulse is reduced due to the relative linewidths of the cavity resonance and pulse spec-

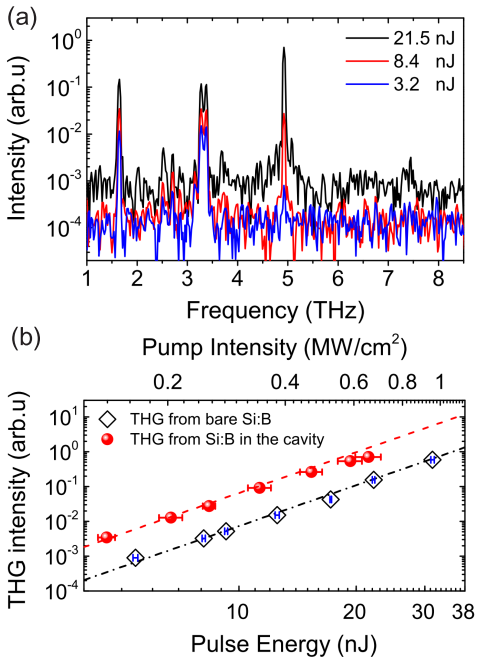

FIG. 4. (a) Measured transmittance/emittance spectra of Si:B in the 1D PC cavity, pumped at three FEL pulse energies of 3.2, 8.4 and 21.5 nJ. (b) Measured intracavity THG intensity as a function of the pump pulse energy (red bullets). For comparison, the THG intensity for free-standing Si:B is shown by the black open diamonds. Dashed red and dash-dotted black lines: Power-law trends with an exponent of 3.9. The horizontal error bars in both data sets indicate the pump power fluctuation during the experiments.

trum (and imperfections of the experimental cavity).

The transmittance of the 1D PC cavity was also experimentally characterized by THz time-domain spectroscopy with a spectral resolution of 5 GHz (dictated by the temporal scan range of 200 ps). The measured transmission spectrum, taken at a temperature of 20 K, is displayed as a blue curve in Fig. 3b. One sees that the cavity resonances coincide with the model calculation, only with some broadening and weakening, which we attribute to imperfect alignment and planarity of the cavity structure. Nevertheless, for the cavity mode at 1.58 THz, the measured FWHM linewidth is 8.8 GHz which translates into a Q-factor of 180. For the THG experiments at 10 K, we first fine-tuned the FEL radiation frequency to best match this cavity mode, i.e. to maximise the transmission (without the high-pass filters in the beam). Note that this occurred at a shifted pump frequency of 1.65 THz, which we attribute to temperature-dependent effects on the cavity geometry compared to the transmission measurement at 20 K.

We performed the FTIR measurements of the transmitted/emitted radiation as per the free-standing sample (Fig. 2), for different pump pulse energies. Fig. 4a shows the measured spectra for 3.2, 8.4 and 21.5 nJ. Again, in addition to the fundamental and second-harmonic signals (at 1.65 THz and 3.30 THz, respectively) which originate from the FEL pump radiation, we observe the THG signal at 4.95 THz (that the residual fourth harmonic from the FEL is no longer measured may be due to the transmission spectrum of the cavity). Again, control measurements with an undoped Si defect layer confirmed that the THG originates from the presence of dopants in the Si:B sample.

Figure 4b displays the intensity of the third harmonic as a function of the pump pulse energy (red bullets), which, as per the free-standing sample, can be fitted with a power-law dependence with the same exponent $\eta = 3.9$ (red dashed line), although at high pump pulse energy (above 15 nJ) some saturation is observed. Hence, we attribute the THG to the same mechanism, i.e. due to free holes which are generated by impact ionization in the THz radiation field. We tend to rule out heating effects for the saturation (Sec. VI C), as these should rather first *increase* the initial residual population of band carriers. However, it is possible that the nonlinear hole current itself exhibits a saturation behavior for large field-driven wavepacket displacement. For a direct comparison of the relative THG intensities obtained with and without the cavity as a function of the pump pulse energy, we present the data of Fig. 2b again in Fig. 4b as black open diamonds. Compared with THG from free-standing Si:B, the intracavity THG yield is increased by a factor of $r = 8$.

We can also estimate the experimental field enhancement r_E of the fundamental pump in the cavity (at the standing-wave antinodes), considering the relative linewidths of the FEL pulses $\Delta\nu_\omega = 22.4$ GHz and cavity resonance $\Delta\nu_c = 8.8$ GHz. We derive the following relation:

$$r = \zeta \cdot (1 + \Delta\nu_p/\Delta\nu_c)^{1-\eta} r_E^{2\eta}, \tag{4}$$

which accounts for the fact that only the central part of the pulse spectrum resonates in the cavity (partially offset by the longer resultant pulse in the cavity) and the standing-wave distribution in the sample $\zeta = \langle \cos^{2\eta} \rangle \approx 0.27$. Solving for the field enhancement yields the value $r_E = 2.5$. This also indicates that the THG enhancement could have been much larger, if the linewidths of the FEL pulses and cavity mode resonance were better matched. If we take $\Delta\nu_p/\Delta\nu_c = 1$ in Eq. (4), we predict a cavity THG enhancement $r = 42$, which rapidly increases to $r \sim 300$ in approaching the CW limit ($\Delta\nu_p \ll \Delta\nu_c$).

IV. DISCUSSION

A. Impact ionization of shallow dopants

We simulated the increase of the density of free holes by impact ionization with Eq. (3), taken from Refs. 26 and 29. There, it was derived for the description of interband (conduction-to-valence-band) transitions by impact processes induced in n-InSb (carrier density: 9.3×10^{12}-2.3×10^{15} cm^{-3}) by 40-ns-long mid-IR pulses[29], respectively in HgTe quantum wells (carrier density: 3×10^{11} cm^{-2}) by 100-ns-long THz pulses[26]. Here, we discuss why this equation should also be applicable for the analysis of our measurements.

Eq. (3) was derived in Refs. 26 and 29 on the basis of the assumption that the carriers are thermalized, having a temperature which is elevated above the lattice temperature by

the action of the radiation field. This assumption is reasonable as the duration of the radiation pulses was much longer than τ, the carrier scattering time, which implies that, during the presence of the pulse, substantial thermalization processes take place among the charge carriers themselves and between charge carriers and lattice, while they continue to be heated by the radiation field. Eq. (3) is based on the picture that carriers in the high-energy Boltzmann tail, which have a kinetic energy larger than the ionization energy U_{ion}, are largely responsible for the carrier multiplication process[35]. In the statistical treatment of the collisions it was assumed that additional ionization by an increased sample (lattice) temperature is significantly weaker and was therefore neglected.

The theoretical treatment of impact ionization in Refs. 26 and 29 also assumes non-thermal contributions to be of secondary significance for the following reason: As the condition $\omega\tau > 1$ holds, the distribution function of the charge carriers in **k**-space is asymmetric; the individual charge carriers draw kinetic energy from the radiation field such that their ensemble-averaged kinetic energy in field direction is higher than away from it. It is now decisive how large this kinetic energy is. Averaged over the radiation cycle, it is approximately given by the ponderomotive energy (see Sec. VI A). As long as this energy is significantly smaller than U_{ion}, it is not a dominant factor in the ionization process.

In our experiments, with τ estimated to be on the order of 2.5 ps[36], much larger than the value of 0.2 ps at room temperature[37,38], one finds that the pulse duration of 23 ps is much longer than τ and that $\omega\tau > 1$, i.e., conditions which are not so different from those of Refs. 26 and 29. Furthermore, the ponderomotive energy U_p of the holes in the driving radiation field is much smaller than the ionization energy. We calculate in the Appendix (Sec. VI A) values of $U_p = 0.93$ meV for the heavy holes and $U_p = 2.9$ meV for the light holes, to be compared with the ionization energy $U_{ion} = 44$ meV. Impact ionization by non-thermal holes hence should be of secondary importance. Taking all aspects together suggests that Eq. (3) should be applicable to our experiments.

We finally recall that impact ionization must fulfill energy and momentum conservation. This is easily possible in the case of ionization of shallow impurities, as a one-dimensional analysis in a parabolic valence band in **k**-space shows. Let $E_1 = \hbar^2 k_1^2/2m$ and $E_1' = \hbar^2 k_1'^2/2m$ be the kinetic energy of a hole before and after the impact interaction with the dopant, and $E_2 = \hbar^2 k_2^2/2m$ the kinetic energy of the second hole after its release from the dopant. Energy conservation requires $E_1 = E_1' + E_2 + U_{ion}$, while momentum conservation demands $k_1 = k_1' + k_2$. With these two equation, one obtains the requirement $k_1' k_2 = m U_{ion}/\hbar^2$ for the final momenta of the two holes which can always be fulfilled, if $E_1 > U_{ion}$.

B. Higher harmonics

As stated in the Introduction, one motivation for this work was the question of whether recollision processes play a role in our solid-state version of a frozen, dilute atomic gas. As a necessary (but not sufficient) indicator for recollision, we considered the appearance of HHG. Revisiting the requirements for the observation of HHG by recollision, we note that the condition for a return of an ionized hole to its ion core is that the motion of the hole is ballistic for at least one oscillation half-cycle of the radiation field. This condition is fulfilled, as $\omega\tau > 1$ (see above in Sec. IV A). A second condition is that the colliding hole acquires enough kinetic energy in the radiation field to emit radiation at higher harmonics of the radiation frequency. From this requirement, we derive a high-frequency cut-off: The highest harmonic number N_c possible is determined by $N_c = \lfloor (U_{ion} + 3.7\,U_p)/(\hbar\omega) \rfloor$ based on semiclassical considerations[9–11]. With the photon energy of 6.45 meV (at 1.56 THz) and the values of U_{ion} and U_p above, one obtains $N_c = 7$ for heavy holes and $N_c = 8$ for light holes. Based on this condition, high harmonics could be generated in our system.

The reason for not observing HHG is probably that the ionization rate is too low to generate a detectable signal. There are, in addition, two factors which may reduce the efficiency or the observability of recollisional HHG further. (i) A tacit assumption of HHG is that the charge carrier is a spatially localized object which is driven away far enough from the potential of the ion core that the recollision process is near-instantaneous. Unlike in gas systems, the holes in our dopant systems are more extended wave-packet objects, the core potential extends further out into space (~ 1 nm) because of the dielectric influence of the host crystal, and the trajectory of the holes brings them not very far away from the ion core (~ 3 nm for heavy holes, 11 nm for light holes). These aspects may lead to a reduction of HHG efficiency. (ii) A possible reason for a suppressed visibility of HHG is the ensemble average of the emission. In the HHG experiments with gases, the ionization and recollision processes of the different atoms are synchronized by the extremely short laser pulses employed. Our experiments were performed with multicycle pulses under conditions where a tight synchronization is not to be expected and destructive interference may be significant.

V. CONCLUSION

By employing intense FEL pulses, we have experimentally demonstrated THG from Si:B at low temperature. The THG process can be attributed to the third-order nonlinearity of free holes in the valence band, where the increase of the susceptibility $\chi^{(3)}$ with pump intensity indicates that the number of free holes also increases due to ionization of the dopants during each pump pulse. While direct tunneling ionization cannot readily account for this intensity dependence, we find that a previously established model for impact ionization, initiated by thermally ionized band carriers, allows us to fit the data over a wide range of pump intensity. In addition, by embedding the Si:B in a 1D PC cavity, we observe an increase in the THG efficiency by up to 8 times compared to the free-standing sample, due to the electric field enhancement at a cavity resonance frequency. A consideration of the relative linewidth of the FEL pump pulses and cavity resonance suggests that the enhancement of intracavity THG efficiency could be in-

creased to a factor exceeding 100 if pump pulses with a narrower linewidth were employed. Such experiments show how dielectric THz cavities, which can be readily constructed with high Q-factor, can greatly enhance nonlinear processes, and can be potentially employed as a platform for many other nonlinear light-matter interaction experiments.

VI. APPENDIX

A. Keldysh parameter

The Keldysh parameter γ is a quantity used in atomic physics to determine, whether multiphoton absorption or tunneling is more efficient at photoionization of gas molecules in strong radiation fields. $\gamma = \sqrt{U_{ion}/(2U_p)}$ compares the ionization energy U_{ion} of the atomic species with the cycle-averaged ponderomotive (quiver) energy $U_p = e^2E_\omega^2/(4m\omega^2)$ of a free electron with mass $m = m_e$. If $\gamma > 1$, multiphoton ionization dominates over tunneling ionization. We evaluate the Keldysh parameter for the case of bound holes in Si:B using the following parameters: $U_{ion} = 44$ meV,[2] effective conductivity mass of light holes $m_{lh} = 0.16\,m_e$ and of heavy holes $m_{hh} = 0.49\,m_e$[39], and $\omega = 2\pi \cdot 1.56$ THz. For a radiation field of $E_\omega = 10$ kV/cm, one obtains a ponderomotive energy of 2.9 meV (0.93 meV) and the value $\gamma = 2.8$ ($\gamma = 4.85$) for light holes (heavy holes).

B. Tunneling ionization rate

An expression for the tunneling rate of holes from acceptors in a strong electric field was derived in Ref. 40 and applied successfully to ionization studies of shallow acceptors in Ge using both DC electric fields[41] and single-cycle THz pulses[42]. There, the tunneling rate of Ref. 40 was approximated by:

$$\tau_i^{-1}(t) = \Omega \left(\frac{6\alpha_E}{E_\omega(t)} \right)^{2n_1^*-1} \exp\left(-\frac{\alpha_E}{E_\omega(t)} \right), \qquad (5)$$

where the parameters Ω, α_E and n_1^* are defined by[41]

$$\Omega = \frac{1}{\sigma^2[\Gamma(n_1^*+1)]^2} \cdot \frac{2U_{ion}}{\hbar}, \qquad (6)$$

$$\alpha_E = \frac{4\sqrt{2m_{lh}}U_{ion}^{3/2}}{3e\hbar}, \qquad (7)$$

$$n_1^* = \frac{e^2}{4\pi\varepsilon_0\varepsilon_r\hbar} \cdot \sqrt{\frac{m_{lh}}{2U_{ion}}}. \qquad (8)$$

$\Gamma(n_1^*+1)$ is the Euler gamma function and $\sigma^2 = 0.63$ a Si valence band parameter[40]. As the tunneling rate increases strongly with decreasing mass, one considers only the light holes here. Using the value of $m_{lh} = 0.16\ m_e$, we arrive at the following values of the three parameters of Eqs. (6)–(8): $\Omega = 2.73 \times 10^{14}$ s^{-1}, $\alpha_E = 261$ kV/cm and $n_1^* = 0.5845$.

With the tunneling rate of Eq. (5), we can derive the density Δn of tunneling-ionized dopants (i.e. the density of additional free holes), generated by each THz pulse by integration over the THz waveform[42]. For weak ionization, i.e., neglecting depletion of the non-ionized dopants: $\Delta n = n_d \int \tau_i^{-1}(t)\,dt$, where n_d is the dopant density, which yields the curve in Fig. 2c. As shown, this leads to values $\Delta n \sim 10^{10}$ cm^{-3} at our peak field of $E = 12$ kV/cm, although there are reports (e.g. for GaAs:C[41]) where it was shown that Eq.s (5-8) can overestimate the experimental tunnel ionization rate by an order of magnitude or so at high fields.

We also remark that pulse-to-pulse accumulation of holes can be ignored, as the time interval between pulses is 76 ns, while the recombination time of holes in Si:B is about 500 ps[43].

C. Thermal carrier concentration and sample heating

One can estimate the density n_0 of thermally ionized holes in the valence band at low temperature T via the relation[44]:

$$n_0 \approx \sqrt{\frac{N_V \cdot n_d}{g_A}} \cdot \exp\left(-\frac{U_{ion}}{2k_BT} \right) \qquad (9)$$

where $n_d = 5 \times 10^{16}$ cm^{-3} is the acceptor concentration, $g_A = 4$ is the degeneracy of the $1\Gamma_+^8$-ground state, and $N_V = 2(2\pi\hat{m}_h kT/h^2)^{3/2}$ is the valence band effective density of states (DOS) in terms of the effective DOS mass $\hat{m}_h = 0.59 \cdot m_e$[44]. For $T = 10$ K, $N_V = 6.9 \times 10^{16}$ cm^{-3}, and one calculates from Eq. (9) a free hole density $n_0 < 10^7$ cm^{-3}, although this rises exponentially to a value $n_0 \sim 10^{11}$ cm^{-3} at $T = 20$ K. Hence the precise residual density of thermally ionized holes (without FEL illumination) depends critically on the actual base temperature of the sample (as well as trace concentrations of compensating donors and other defects) and is difficult to quantify. However, our main aim here is to evaluate whether the Drude absorption of these carriers should lead to a significant temperature increase of the sample (and hence further thermal ionization) under the steady-state FEL illumination, with a maximum energy of $J_\omega \sim 30$ nJ and average power of $\bar{P}_\omega \sim 390$ mW.

The Drude absorption coefficient (for weak absorption and a scattering time τ such that $\omega\tau \gg 1$) is given by

$$\alpha \approx \frac{n_0 e^2}{\varepsilon_0 c_0 \sqrt{\varepsilon_{\infty r}} \cdot m_h \omega^2 \tau}, \qquad (10)$$

where $\varepsilon_{\infty r} = 11.8$ is the background relative permittivity and $m_h = 0.345 \cdot m_e$ the effective hole conductivity mass[45]. If we assume a relatively high nominal density of $n_0 = 10^{12}$ cm^{-3} and $\tau = 1$ ps (so as not to underestimate beam absorption and heating), then the absorption coefficient in Eq. (10) still amounts to only $\alpha \sim 10^{-4}$ mm^{-1}.

Considering first the initial temperature rise ΔT_1 on the beam axis due to a single pump pulse, with the THz focal $1/e^2$-beam diameter $2w = 400\ \mu$m. The deposited heat density is $u_1(r=0) = \alpha J_\omega/(\frac{1}{2}\pi w^2)$, and so $\Delta T_1 = u_1/c_V$ where $c_V = c\rho = 7 \times 10^{-4}$ J cm^{-3} K^{-1} is the volumetric heat capacity

at 10 K,[46] from which we calculate $\Delta T_1 \sim 100\ \mu$K, i.e. negligible heating. Nevertheless, one must also evaluate the accumulated steady-state temperature rise ΔT in the train of such pulses (repetition rate $\nu_p = 13$ MHz). Here one must account for the edge cooling of the sample which occurs at the perimeter of the circular metallic mounting aperture with inner diameter $2R = 6$ mm (while radiative cooling can be shown to be negligible). As $\alpha L \ll 1$ (sample thickness $L = 275\ \mu$m), the heating should be approximately uniform along the beam axis. Hence one can solve the radially symmetric steady-state 2D heat diffusion equation $\nabla_r^2 T = -\alpha \bar{I}_\omega(r)/k_T$ with the boundary condition $\Delta T(r = R) = 0$, where the average THz intensity $\bar{I}_\omega(r) = \bar{P}_\omega/(\frac{1}{2}\pi w^2)e^{-2r^2/w^2}$ and the thermal conductivity $k_T = 7\,\mathrm{W\,cm^{-1}\,K^{-1}}$ (at 10 K)[47]. The solution can be derived as $\Delta T(r = 0) = \alpha P \eta/(2\pi k)$,[48] where $\eta(w,R) = 3.3$ is a geometric factor. With the heat diffusion coefficient $\beta = k/c_V = 1\ \mathrm{m^2\ s^{-1}}$, we find $\Delta T(r = 0)/\Delta T_1 = \nu_p w^2/(4\beta) \sim 1$, i.e. also no significant steady-state heating, this due to the fact that the characteristic diffusion time $w^2/(4\beta)$ is on the order of the inter-pulse period. Hence we can neglect beam heating effects on the residual free hole density vs. FEL pump intensity in the range studied in this paper.

ACKNOWLEDGMENTS

Funding by DFG under contract RO 770/41 is gratefully acknowledged. Parts of this research were carried out at the ELBE Center for High-Power Radiation Sources; for more information about the facility, see DOI: 10.17815/jlsrf-2-58. The authors thank P. Michel and the FELBE team at HZDR for their dedicated support, and Wu Dai for assistance during some of the experiments. The supplementary measurements and support from the TELBE team are acknowledged.

[1] N. Sclar and E. Burstein, "Optical and impact recombination in impurity photoconductivity in germanium and silicon," Phys. Rev. **98**, 1757–1760 (1955).

[2] A. Onton, P. Fisher, and A. K. Ramdas, "Spectroscopic investigation of group-III acceptor states in silicon," Phys. Rev. **163**, 686–703 (1967).

[3] M. A. W. van Loon, N. Stavrias, N. H. Le, K. L. Litvinenko, P. T. Greenland, C. R. Pidgeon, K. Saeedi, B. Redlich, G. Aeppli, and B. N. Murdin, "Giant multiphoton absorption for THz resonances in silicon hydrogenic donors," Nat. Photonics **12**, 179–184 (2018).

[4] N. H. Le, G. V. Lanskii, G. Aeppli, and B. N. Murdin, "Giant non-linear susceptibility of hydrogenic donors in silicon and germanium," Light Sci. Appl. **8**, 64 (2019).

[5] S. G. Pavlov, N. Deßmann, V. N. Shastin, R. K. Zhukavin, B. Redlich, A. F. G. van der Meer, M. Mittendorff, S. Winnerl, N. V. Abrosimov, H. Riemann, and H.-W. Hübers, "Terahertz stimulated emission from silicon doped by hydrogenlike acceptors," Phys. Rev. X **4**, 021009 (2014).

[6] P. T. Greenland, S. A. Lynch, , A. F. G. van der Meer, B. N. Murdin, C. R. Pidgeon, B. Redlich, N. Q. Vinh, and G. Aeppli, "Coherent control of Rydberg states in silicon," Nature **465**, 1057–1062 (2010).

[7] K. Litvinenko, E. Bowyer, P. Greenland, N. Stavrias, J. Li, R. Gwilliam, B. Villis, G. Matmon, M. Pang, B. Redlich, A. van der Meer, C. Pidgeon, G. Aeppli, and B. Murdin, "Coherent creation and destruction of orbital wavepackets in Si:P with electrical and optical read-out," Nat. Commun. **6**, 6549 (2015).

[8] F. Krausz and M. Ivanov, "Attosecond physics," Rev. Mod. Phys. **81**, 163–234 (2009).

[9] T. Brabec and F. Krausz, "Intense few-cycle laser fields: Frontiers of nonlinear optics," Rev. Mod. Phys. **72**, 545–591 (2000).

[10] M. Lewenstein, P. Balcou, M. Y. Ivanov, A. L'Huillier, and P. B. Corkum, "Theory of high-harmonic generation by low-frequency laser fields," Phys. Rev. A **49**, 2117–2132 (1994).

[11] J. L. Krause, K. J. Schafer, and K. C. Kulander, "High-order harmonic generation from atoms and ions in the high intensity regime," Phys. Rev. Lett. **68**, 3535–3538 (1992).

[12] M. Ferray, A. L'Huillier, X. F. Li, L. A. Lompré, G. Mainfray, and C. Manus, "Multiple-harmonic conversion of 1064 nm radiation in rare gases," J. Phys. B: At. Mol. Opt. Phys. **21**, L31–L35 (1988).

[13] T. Chen, P. Liu, J. Liu, and Z. Hong, "A terahertz photonic crystal cavity with high q-factors," Appl. Phys. B **115**, 105–109 (2014).

[14] Q. Zhang, M. Lou, X. Li, J. L. Reno, W. Pan, J. D. Watson, M. J. Manfra, and J. Kono, "Collective non-perturbative coupling of 2d electrons with high-quality-factor terahertz cavity photons," Nat. Phys. **12**, 1005–1011 (2016).

[15] F. Meng, M. D. Thomson, B. Klug, D. Čibiraitė, Q. Ul-Islam, and H. G. Roskos, "Nonlocal collective ultrastrong interaction of plasmonic metamaterials and photons in a terahertz photonic crystal cavity," Opt. Express **27**, 24455–24468 (2019).

[16] R. N. Bhatt, "Shallow impurity interactions and the metal-insulator transition," Physica **146B**, 99–111 (1987).

[17] G. A. Thomas, M. Capizzi, F. DeRosa, R. N. Bhatt, and T. M. Rice, "Optical study of interacting donors in semiconductors," Phys. Rev. B **23**, 5472–5494 (1981).

[18] H. J. Hrostowski and R. H. Kaiser, "Infrared spectra of group III acceptors in silicon," J. Phys. Chem. Solids **4**, 148–153 (1958).

[19] J. J. Wynne and G. D. Boyd, "Study of optical difference mixing in Ge and Si using a CO_2 gas laser," Appl. Phys. Lett. **12**, 191–192 (1968).

[20] A. Mayer and F. Keilmann, "Far-infrared nonlinear optics. ii. $\chi^{(3)}$ contributions from the dynamics of free carriers in semiconductors," Phys. Rev. B **33**, 6962–6968 (1986).

[21] M. D. Thomson, M. Kreß, T. Löffler, and H. G. Roskos, "Broadband THz emission from gas plasmas induced by femtosecond optical pulses: From fundamentals to applications," Laser Photon. Rev. **1**, 349–368 (2007).

[22] S.Žurauskas and A. Dargys, "Field ionization of phosphorus atoms in silicon," phys. stat. sol. (b) **121**, 385–391 (1984).

[23] S. H. Koenig, R. D. Brown III, and W. Schillinger, "Electrical conduction in n-type germanium at low temperatures," Phys. Rev. **128**, 1668–1696 (1962).

[24] N. Sclar and E. Burstein, "Impact ionization of impurities in germanium," J. Phys. Chem. Solids **2**, 1–23 (1957).

[25] The literature reports investigations of the ionization of deep impurities in intense infrared radiation fields. There, phonon-assisted tunneling and the Poole-Frenkel effect dominate the ionization[49,50]. The ionization rates of those two ionization scenarios are independent of the pump frequency[50]. In our experiments, we noticed that the ionization rate increased as the pump frequency decreased, which is consistent with the prediction of impact ionization as opposed to phonon-assisted tunneling and the Pool-Frenkel effect.

[26] S. Hubmann, S. Gebert, G. V. Budkin, V. V. Bel'kov, E. L. Ivchenko, A. P. Dmitriev, S. Baumann, M. Otteneder, J. Ziegler, D. Disterheft, D. A. Kozlov, N. N. Mikhailov, S. A. Dvoretsky, Z. D. Kvon, D. Weiss, and S. D. Ganichev, "High-frequency impact ionization and nonlinearity of photocurrent induced by intense terahertz radiation in hgte-based quantum well structures," Phys. Rev. B **99**, 085312 (2019).

[27] H. Hirori, K. Shinokita, M. Shirai, S. Tani, Y. Kadoya, and K. Tanaka, "Extraordinary carrier multiplication gated by a picosecond electric field pulse," Nat. Commun. **2**, 594 (2011).

[28] H. Wen, M. Wiczer, , and A. M. Lindenberg, "Ultrafast electron cascades in semiconductors driven by intense femtosecond terahertz pulses," Phys. Rev. B **78**, 125203 (2008).

[29] S. D. Ganichev, A. P. Dmitriev, S. A. Emel'yanov, Y. V. Terent'ev, I. D. Yaroshetskii, and I. N. Yassievich, "Impact ionization in semiconductors under the influence of the electric field of an optical wave," Sov. Phys. JETP **63**, 256–263 (1986).

[30] H. A. Hafez, S. Kovalev, J.-C. Deinert, Z. Mics, B. Green, N. Awari, M. Chen, S. Germanskiy, U. Lehnert, J. Teichert, Z. Wang, K.-J. Tielrooij, Z. Liu, Z. Chen, A. Narita, K. Müllen, M. Bonn, M. Gensch, and D. Turchinovich, "Extremely efficient terahertz high-harmonic generation in graphene by hot dirac fermions," Nature **561**, 507–511 (2018).

[31] W. Kuehn, P. Gaal, K. Reimann, M. Woerner, T. Elsaesser, and R. Hey,

"Coherent ballistic motion of electrons in a periodic potential," Phys. Rev. Lett. **104**, 146602 (2010).
[32]P. A. Wolff and G. A. Pearson, "Theory of optical mixing by mobile carriers in semiconductors," Phys. Rev. Lett. **17**, 1015–1017 (1966).
[33]C. K. N. Patel, R. E. Slusher, and P. A. Fleury, "Optical nonlinearities due to mobile carriers in semiconductors," Phys. Rev. Lett. **17**, 1011–1014 (1966).
[34]M. Woerner and T. Elsaesser, "Ultrafast thermalization of nonequilibrium holes in p-type tetrahedral semiconductors," Phys. Rev. B **51**, 17490–17498 (1995).
[35]Note, that the situation treated in Refs. 26 is more complex than just described because the Fermi energy of the carrier distribution lies above the conduction band edge, and freeing states for re-population plays a major role.
[36]P. J. Morin and J. P. Maita, "Electrical properties of silicon containing arsenic and boron," Phys. Rev **96**, 28–35 (1954).
[37]F. Meng, M. D. Thomson, B. E. Sernelius, M. Jörger, and H. G. Roskos, "Ultrafast dynamic conductivity and scattering rate saturation of photoexcited charge carriers in silicon investigated with a midinfrared continuum probe," Phys. Rev. **91**, 075201 (2015).
[38]M. Woerner, W. Frey, M. T. Portella, C. Ludwig, T. Elsaesser, and W. Kaiser, "Ultrafast thermalization of nonequilibrium holes in p-type germanium studied by femtosecond infrared spectroscopy," Phys. Rev. B **49**, 17007–17010 (1994).
[39]"Physical properties of Si," `http://www.ioffe.ru/SVA/NSM/Semicond/Si/`.
[40]H. Q. Nie and D. Coon, "Tunneling of holes from acceptor levels in an applied field," Solid State Electron. **27**, 53–58 (1984).
[41]A. Dargys and S. Žurauskas, "Tunnel ionization of shallow acceptors and donors in GaAs," J. Phys.: Condens. Matter **7**, 2133–2146 (1995).
[42]Y. Mukai, H. Hirori, and K. Tanaka, "Electric field ionization of gallium acceptors in germanium induced by single-cycle terahertz pulses," Phys. Rev. B **87**, 201202(R) (2013).
[43]N. Q. Vinh, B. Redlich, A. F. G. van der Meer, C. R. Pidgeon, P. T. Greenland, S. A. Lynch, G. Aeppli, and B. N. Murdin, "Time-resolved dynamics of shallow acceptor transitions in silicon," Phys. Rev. X **3**, 011019 (2013).
[44]R. F. Pierret, Advanced Semiconductor Fundamentals, 2nd ed. (Pearson Education Inc., New Jersey, 2002).
[45]D. M. Riffe, "Temperature dependence of silicon carrier effective masses with application to femtosecond reflectivity measurements," J. Opt. Soc. Am. B **19**, 1092–1100 (2002).
[46]P. Flubacher, A. J. Leadbetter, and J. A. Morrison, "The heat capacity of pure silicon and germanium and properties of their vibrational frequency spectra," Phil. Mag. **4**, 273–294 (1959).
[47]C. J. Glassbrennert and G. A. Slack, "Thermal conductivity of silicon and germanium from 3K to the melting point," Phys. Rev. **134**, A1058–A1069 (1964).
[48]C. A. Klein, "Beam-induced spherical aberration in cooled cw laser light transmitting components," in Laser Induced Damage in Optical Mateials: 1986, NIST Special Publication 752 (National Institute of Standards and Technology, Washington DC, 1988) pp. 96–126.
[49]S. Ganichev, "Tunnel ionization of deep impurities in semiconductors induced by terahertz electric fields," Physica B **273-274**, 737–742 (1999).
[50]S. D. Ganichev, E. Ziemann, W. Prettl, I. N. Yassievich, A. A. Istratov, and E. R. Weber, "Distinction between the Poole-Frenkel and tunneling models of electric-field-stimulated carrier emission from deep levels in semiconductors," Phys. Rev. B **61**, 10361–10365 (2000).